Computer modelling of $Hg_{1-x}Cd_xTe$ photodiode performance

Robert Ciupa*

Abstract

A numerical technique has been used to solve the carrier transport equations for $Hg_{1-x}Cd_xTe$ photodiodes. The model allows a calculation of the spatial distribution of the electric field, the electron and hole concentrations and the generation-recombination rate. This was used to analyse the influence of the base region length and the effect of doping profiles on the photodiode parameters (R_oA product, current responsivity and detectivity). It was found that the R_oA product is controlled by diffusion limited mechanism.

Introduction

In the recent several years, the unquestionable leader among semiconductor materials used in the production of infrared detectors has been mercury-cadmium telluride. Particular interest in this material results, first of all, from its fundamental physical properties. It is characterized by variable, composition-dependent energy bandgap. It demonstrates high mobility of electrons in relation to the mobility of holes and has low permittivity, as well as the possibility to produce both low and high concentrations of majority carriers. Small variation in the lattice constant with variation in composition enables one to obtain high-quality thin films and heterostructures. $Hg_{1-x}Cd_xTe$ detectors operate over a wide range of temperatures (77K - 300K). They can be tuned in a very wide spectral region (1–30μm). This is a very well known material and if one considers narrow bandgap semiconductors, it is probably the one that is most comprehensively described in the literature at the present time [1 - 3].

The quality of the material has reached the level required for construction of multi-element arrays and lines, but it is also the most technologically difficult of all semiconductor materials when applied to industrial production. The basic problems are: difficulties in obtaining homogeneous material, difficulties in obtaining reproducible parameters, and high costs of production. The main reason for this situation is the weakness of the mercury bonding in the compound. This causes lattice and surface instabilities of $Hg_{1-x}Cd_xTe$ which, as a consequence, influences degradation of devices constructed from this material.

Numerical analysis

The properties of a photodiode can be modelled by taking account of the set of five differential equations, i.e.:

– two phenomenological transport equations for electrons and holes

* Military University of Technology, Institute of Applied Physics, 2 Kaliskiego St., 00-908 Warsaw, Poland

$$J_h = -qD_h \frac{dp}{dx} - q\mu_h p \frac{d\Psi}{dx} \quad (1)$$

$$J_e = qD_e \frac{dn}{dx} - q\mu_e n \frac{d\Psi}{dx} \quad (2)$$

– two continuity equations

$$\frac{dJ_e}{dx} + q(G-R) = 0 \quad (3)$$

$$\frac{dJ_h}{dx} - q(G-R) = 0 \quad (4)$$

and

– Poisson's equation

$$\frac{d^2\Psi}{dx^2} = -\frac{q}{\varepsilon_s \varepsilon_o}(N_d - N_a + p - n) \quad (5)$$

where n, D_e, μ_e and J_e are the electron concentration, diffusion coefficient, mobility and current density, respectively, p, D_h, μ_h and J_h are corresponding quantities for holes, q is the electron charge, G and R are the generation and recombination rates, respectively, Ψ is the electric potential, N_d and N_a are the donor and acceptor concentrations, respectively, ε_s is the static dielectric function, and ε_o is the permittivity of free space.

In the vicinity of room temperature, the thermal generation and recombination rates are determined by the Auger 1 and Auger 7 processes. The corresponding net generation rate (the difference between generation and recombination rates) is

$$G_A - R_A = \frac{n_i^2 - np}{2n_i^2}\left(\frac{n}{(1+an)\tau_{A1}^i} + \frac{p}{\tau_{A7}^i}\right) \quad (6)$$

where τ_{A1}^i and τ_{A7}^i are the intrinsic Auger 1 and Auger 7 recombination times, and n_i is the intrinsic concentration. The finite value of *a* results from the degeneracy of heavily doped n-type material. According to Ref. [4], $a = 5.26\times10^{-18}$ cm^{-3}. By contrast, due to the shape of the valence band, the degeneracy in the p-type material occurs only at a very high doping level that is not achievable in practice.

The intrinsic recombination time can be expressed as

$$\tau_{A1}^i = \frac{3.8*10^{-18}\varepsilon_s^2(1+m_e^*)^{1/2}(1+2m_e^2/m_h^*)}{\frac{m_e^*}{m_h^*}[F_1F_2]^2\left(\frac{kT}{E_g}\right)^{3/2}} * \exp\left(\frac{1+2m_e^*/m_h^*}{1+m_e^*/m_h^*} * \frac{E_g}{kT}\right) \quad (7)$$

where $[F_1F_2]$ is the overlap integral of periodic parts of Bloch functions. The value of $[F_1F_2] = 0.2$ will be used in the following calculations.
The ratio of the Auger 7 and Auger 1 intrinsic recombination times is [5,6].

$$\frac{\tau_{A7}^{i}}{\tau_{A1}^{i}} = \frac{6(1-5E_g/4kT)}{1-3E_g/2kT} \tag{8}$$

The differential equations (1–5) have been solved numerically. As a result, the fundamental variables, p, n, and Ψ, as a function of the position have been computed, thereby enabling an analysis of the photoelectric properties of the device.

The current responsivity, R_i, of the photodiode is the ratio of the photocurrent and the radiation power, P_o. It can be calculated assuming the total generation rate, G, in Eqns. (3, 4) as the sum of the thermal and optical generation rates and calculating the increase in the total current. The position-dependent optical generation rate, $G_o(x)$, has been calculated from

$$G_o(x) = \frac{P_o(1-r_1)}{A_o}\frac{\lambda \exp(-\alpha x)}{hc} \tag{10}$$

where r_1 is the front-surface reflectivity and A_o is the optical area. The back-surface reflectivity is assumed equal to 0. The absorption coefficient, α, has been calculated using the Anderson expressions [7] derived from the Kane model [8] and taking into account the Moss-Burstein bandfilling effect.

The noise current of the device results from the statistical nature of generation and recombination processes. It can be expressed as [9]

$$I_n^2 = \int_0^t 2q^2(G+R)A_e g^2 \Delta f dx \tag{11}$$

where t is the detector thickness, g is the photoelectric gain, A_e is the electrical area of the detector, and Δf is the electrical bandwidth of the receiver.

It should be noted that the effects of fluctuating recombination rate can be frequently avoided by arranging for the recombination process to take place in a region of the device where it has little effect due to low photoelectric gain; for example, at the contacts in sweep-out photoconductors or in the neutral regions of diodes. The generation process with its associated fluctuation, however, cannot be avoided by any means.

The detectivity can be calculated as

$$D^* = \frac{R_i(A\Delta f)^{1/2}}{I_n} \tag{12}$$

In order to undertake a dc steady-state numerical analysis, the current density equations for electrons and holes, the continuity equations for electrons and holes and Poisson's equation were transformed into difference equations in which the variables were defined at a finite number of division points. The meshpoint spacing was defined as a function of the space coordinate x. The choice of fine spacing for a high-field depletion layer and a coarse spacing for a neutral region was preferable.

Practically, the meshpoint spacing from 5×10^{-8} m to 2×10^{-7} m had been used. The quantities of current density, generation and recombination rates are non-linear functions and they are linearized by the Taylor expansion regarding fundamental variables p, n and the electric potential, with neglecting of higher-order terms. The solution of the original differential equations is then replaced by that of the matrix vector equation. The method can be related to as the Newton iteration procedure.

Results and discussion

Using the results of analyses carried out in numerous papers [10 - 14], one can expect that the best parameters of detectors manufactured from these compounds should be obtained for the n^+–p structure. Such a structure is shown in Fig. 1. The role of the n^+ layer is limited to merely formation of the junction. Due to a strong degeneration and the short diffusion length of minority carriers, usually generation in this region makes a small contribution to the dark current and the diode noise. Moreover, due to a strong Burstein-Moss effect, absorption of radiation in this region is very small.

The thicker p-type region is an absorber of infrared radiation. In order to attain the high quantum efficiency close to unity, the condition of longer diffusion length of minority carriers than the radiation penetration depth ($L_D > 1/\alpha$) have to be fulfilled. This can be easily achieved in cryogenically cooled devices. The situation with near room temperature devices is quite different. In contrast to the low temperature case, the diffusion length at high temperature is low and the absorption of IR radiation weak

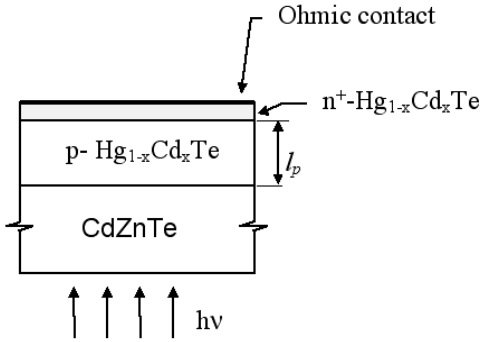

Figure 1. Structure of n^+–p photodiode.

In optimally constructed photodiodes, one tends to obtain the best possible quantum efficiency with the dark current as low as possible. These two parameters demonstrate the opposite direction of variations with variation in, e.g., the energy gap bandwidth or the base region thickness, therefore the normalised detectivity of the photodiode should attain its maximum value only for a strictly defined construction. Thus, it is important to determine precisely the thickness of the active region, the doping profile and the energy bandwidth. The approximate value of doping level can be easily determined using the simple theory ($p = \gamma^{1/2} n_i$ for the condition of minimum thermal Auger generation) but, unfortunately, determination of the energy bandwidth and the base-region thickness, particularly for higher operating temperatures of the detector, requires accurate numerical calculations.

The base region (Fig. 1) with thickness less than the diffusion length for minority carriers should be limited with a surface of low recombination rate. This is accomplished by the creating the diode structure on a substrate of much broader

energy bandgap, with a contact at the p-type side located at a position that is far away from the junction.

a) b)

Figure 2. The dependence of the R_oA product on thickness of p-type regions $Hg_{1-x}Cd_xTe$ photodiode for optimal acceptor concentration of the base region: a) $N_a = 10^{15}$ cm^{-3} ($\lambda = 5\mu$m), b) $N_a = 2\times10^{16}$ cm^{-3} ($\lambda = 8$ μm).

Figure 2 shows the calculated R_oA product as a function of thickness of p-type regions n^+-p $Hg_{1-x}Cd_xTe$ photodiode at 220 K. Acceptor concentration of the base region should be $p = \gamma^{1/2}n_i$ for the condition of minimum thermal Auger generation. R_oA product decreases with thickness increasing of the base p-type region. In the case of photodiodes operating at 5μm (Fig. 2a) this function is linear because the diffusion length of minority carriers is longer than the length of p-type region. This condition is not fulfilled in the photodiodes operating at 8 μm (Fig. 2b). In this case the R_oA product is a sum of a junction and series resistance.

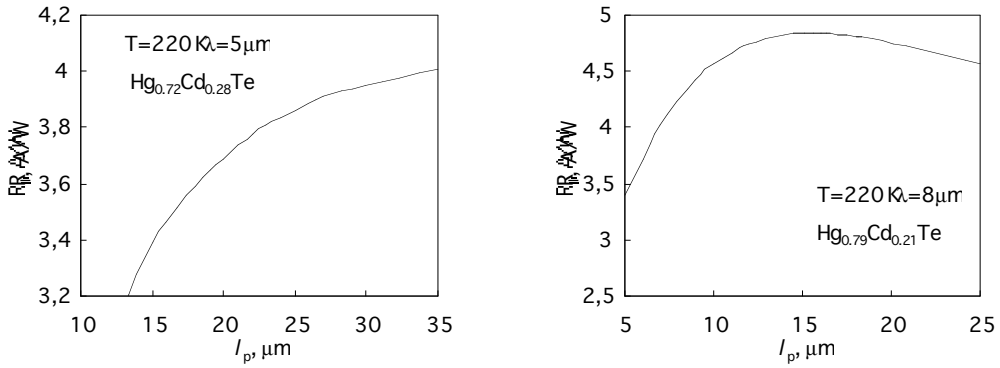

a) b)

Figure 3. The dependence of the current responsivity on thickness of p-type regions n^+-p $Hg_{1-x}Cd_xTe$ photodiode for optimal acceptor concentration of the base region: a) $N_a = 10^{15}$ cm^{-3} ($\lambda = 5\mu$m), b) $N_a = 2\times10^{16}$ cm^{-3} ($\lambda = 8\mu$m).

Figure 3 shows dependence of the current responsivity on thickness of p-type region n^+-p $Hg_{1-x}Cd_xTe$ photodiode for optimal acceptor concentration of the base region. The responsivity increases with thickness increasing of the base p-type region. For $Hg_{1-x}Cd_xTe$ photodiode operating at 8μm (Fig. 3b) this curve increases only for the length of the base region less then 16μm. For greater length of p-type region, diffusion length of minority carriers and the radiation penetration depth are too short

to achieve junction by all optical generated carriers. In the consequence the responsivity decreases with thickness increasing.

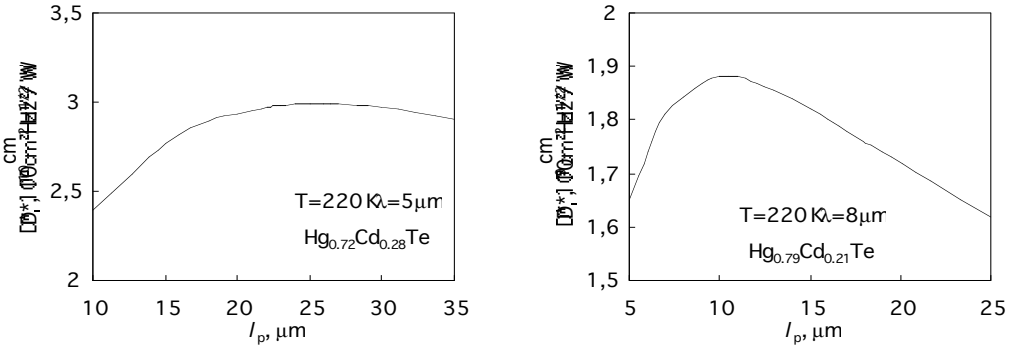

a) b)

Figure 4. Detectivity vs. thickness of p- regions n^+-p $Hg_{1-x}Cd_xTe$ photodiode for optimal acceptor concentration of the base region:
a) $N_a = 10^{15}$ cm^{-3} ($\lambda = 5\mu m$), b) $N_a = 2\times10^{16}$ cm^{-3} ($\lambda = 8$ μm).

Figure 4 shows dependence of the normalised detectivity on thickness of p-type region n^+-p $Hg_{1-x}Cd_xTe$ photodiodes for optimal acceptor concentration of the base region. The detectivity is proportional to $(R_0A)^{1/2}$ and R_I [18]. These two parameters demonstrate the opposite direction of variations with variation of the base region thickness, therefore the normalised detectivity of the photodiode should attain a maximum. It is clearly shown in figure 4 but in analysed range of changes of thickness, normalised detectivity changes a little.

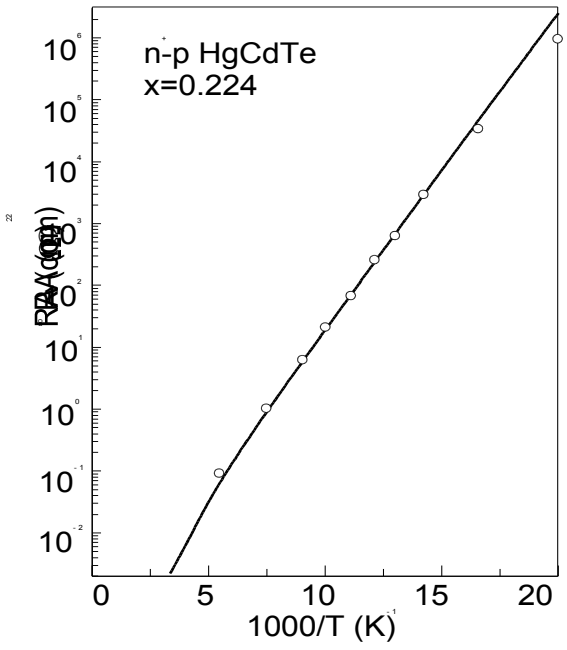

Figure 5. Temperature dependence of the R_0A product of n^+-p. $Hg_{0.776}Cd_{0.224}Te$. Experimental data were taken from [15].
Figure 5 shows temperature dependence of the R_0A product of n^+-p $Hg_{0.776}Cd_{0.224}Te$. Experimental data were taken from [15]. We can see a good agreement between the experimental points and the theoretical curve (solid line).

Conclusions

It results from the calculations carried out that the detectivity possible to be attained in the $Hg_{1-x}Cd_xTe$ structures under analysis is comparable with the detectivity achieved in photoresistors operating in the similar conditions [16]. The photodiodes, however, have valuable advantages: they do not require any supply, which limits power dissipation, and they are characterised by much higher rate of operation. The application of the structure on the substrate of broadened energy bandgap causes about two-times increase in its detectivity, and the application of a thermoelectric cooler leads to further, about five-time, increase in the value of this parameter. It results from the calculations performed that the optimum photodiode parameters—such as thickness and doping—are different for the structure on the substrate with broadened energy bandgap and for the construction with ohmic contacts on its both ends. The calculations carried out have been also confirmed recently by experimental results [17].

Further improvement in parameters of the long-wavelength photodiode operating at near-room temperature can be achieved by the application of optical immersion [18,19]. Optical immersion of a detector in a hemi- or hyperhemispherical lens results in an apparent increase in the linear size by a factor equal to n and n^2, respectively, where n is the refractive index of the immersion lens. This optical effect causes an increase in the resistivity and voltage responsivity by a factor of n^2 and n, respectively[18,19]. Immediate improvement in the detectivity by a factor of n and n^2, respectively, occurs.

Thanks to the rather simple structure analysed in this paper (Fig. 1) we used the 1-D equations which were found to be quite satisfactory in this case. However, usually the photodetector structures are more complicated which forces to use 2 or 3-D equations. Additionally dependence on time may be found to be important. 2 or 3-D time-space cases cause a large complicate of the finite difference solution. It is possible that the use of the Transmission Line Matrix (TLM) method of analysis of detector performance can facilitate the calculation. However this problem needs a separate paper since the comprehensive application of TLM in semiconductor devices does not appear to have been addressed yet.

References

1. D. Long, J.L. Schmit, *Mercury-Cadmium Telluride and Closely Related Alloys*, in "Semiconductors and Semimetals", edited by R.K. Willardson and A.C. Beer, Academic Press, New York, 1970.
2. E. Finkman, Y. Nemirovsky, J. Appl, Phys. **59** (1986) 1205
3. P. Capper, J. Vac. Sci. Technol. **B9** (1991) 1667
4. A.M. White, *The characteristics of minority-carrier exclusion in narrow direct gap semiconductors* Infrared Phys. **25** (1985) 729
5. T.N. Casselman and P.E. Peterson, *A comparison of the dominant Auger transitions in p-type (Hg,Cd)Te* Solid State Comms. **33** (1980) 615
6. T.N. Casselman, *Calculation of the Auger lifetime in p-type* $Hg_{1-x}Cd_xTe$ J. Appl. Phys. **52** (1981) 848
7. W.W. Anderson, *Absorption constant of* $Pb_{1-x}Sn_xTe$ *and* $Hg_{1-x}Cd_xTe$ *alloys* Infrared Phys. **20** (1980) 363
8. E.O. Kane, *Band structure of InSb* J. Phys. Chem. Solids **1** (1980) 249
9. A. Rose, *Concepts in Photoconductivity and Allied Problems* Interscience Publishers, New York, 1963
10. J. Piotrowski and R. Ciupa, *Theoretical performance of near room temperature long wavelength IR photovoltaic detectors* Proc. SPIE **2373** (1995) 388
11. R. Ciupa, Doctoral thesis, Warsaw, 1998 (in Polish)
12. A. Rogalski and R. Ciupa, *Long-wavelength HgCdTe photodiodes:* n^+*-on-p versus p-on-n structures* J. Appl. Phys. **77** (1995) 3505
13. A. Rogalski and R. Ciupa, *Theoretical modeling of long-wavelength* n^+*-on-p HgCdTe photodiodes* J. Appl. Phys. **80** (1996) 2483
14. T. Niedziela and R. Ciupa, *Optimisation of Parameters of (Cd.,Hg)Te* n^+*–p Photodiodes for 10.6μm Spectral Region Operating at Near-Room Temperature* Electron Technology, **33** (2000) 4
15. G. Destefanis and F.P. Chamonal J. Elect. Mater. **22** (1993) 1027
16. J.E. Slavek and H.H. Randal, *Optical immersion of HgCdTe photoconductive detectors* Infrared Phys. **15** (1975) 339–340
17. M. Grudzieñ and J. Piotrowski, *Monolithic optically immersed HgCdTe IR detectors* Infrared Phys. **29** (1989) 251–253
18. J. Piotrowski, $Hg_{1-x}Cd_xTe$ *photodetectors*, chapter 11 in "Infrared Photon Detectors", edited by A. Rogalski, SPIE Optical Engineering Press, Bellingham, Washington, USA (1995).
19. J. Piotrowski and W. Gawron, *Extension on long wavelength IR photovoltaic detector operation to near room temperatures* Infrared Phys. **38** (1997) 63